ORIGINAL ARTICLE

Myocd regulates airway smooth muscle cell remodeling in response to chronic asthmatic injury

Qin Yang[1,2], Qing Miao[1], Hui Chen[1,3], Duo Li[1], Yongfeng Luo[1], Joanne Chiu[1], Hong-Jun Wang[1,3],
Michael Chuvanjyan[1], Michael S Parmacek[4] and Wei Shi[1,3]* ![ORCID]

[1] Department of Surgery, Children's Hospital Los Angeles, Keck School of Medicine, University of Southern California, Los Angeles, CA, USA
[2] Department of Respiratory Medicine, Shenzhen Children's Hospital, Shenzhen, PR China
[3] Division of Pulmonary, Critical Care and Sleep Medicine, Department of Internal Medicine, University of Cincinnati College of Medicine, Cincinnati, OH, USA
[4] Department of Medicine, Perelman School of Medicine, University of Pennsylvania, Philadelphia, PA, USA

*Correspondence to: W Shi, University of Cincinnati College of Medicine, 231 Albert Sabin Way, ML0564, Cincinnati, OH 45267, USA.
E-mail: shiwe@ucmail.uc.edu

Abstract

Abnormal growth of airway smooth muscle cells is one of the key features in asthmatic airway remodeling, which is associated with asthma severity. The mechanisms underlying inappropriate airway smooth muscle cell growth in asthma remain largely unknown. Myocd has been reported to act as a key transcriptional coactivator in promoting airway–specific smooth muscle development in fetal lungs. Whether Myocd controls airway smooth muscle remodeling in asthma has not been investigated. Mice with lung mesenchyme–specific deletion of *Myocd* after lung development were generated, and a chronic asthma model was established by sensitizing and challenging the mice with ovalbumin for a prolonged period. Comparison of the asthmatic pathology between the *Myocd* knockout mice and the wild–type controls revealed that abrogation of Myocd mitigated airway smooth muscle cell hypertrophy and hyperplasia, accompanied by reduced peri–airway inflammation, decreased fibrillar collagen deposition on airway walls, and attenuation of abnormal mucin production in airway epithelial cells. Our study indicates that Myocd is a key transcriptional coactivator involved in asthma airway remodeling. Inhibition of Myocd in asthmatic airways may be an effective approach to breaking the vicious cycle of asthmatic progression, providing a novel strategy in treating severe and persistent asthma.
© 2022 The Authors. *The Journal of Pathology* published by John Wiley & Sons Ltd on behalf of The Pathological Society of Great Britain and Ireland.

Introduction

Asthma is an inflammatory disease of airways, and the resultant airway structural changes, including both cellular and extracellular compartments, are referred to as airway remodeling. Airway remodeling is a typical pathological feature of asthma and can lead to exacerbated airway hyperresponsiveness, airflow limitation, and eventually irreversible decrease of pulmonary function [1]. Airway remodeling can start early in childhood asthma and continue into adulthood, becoming the major cause of refractory asthma and asthma-related mortality [2,3]. Therefore, preventing and reversing airway remodeling is as important as inhibiting airway inflammation for the treatment of asthma [4].

During asthmatic inflammation, a variety of factors, including proinflammatory cytokines and neurotransmitters, act on smooth muscle cells of airway medial walls to induce proliferation and hypertrophy [5]. The abnormal growth of these airway smooth muscle cells (ASMCs) is one of the major pathological changes observed in asthmatic airway remodeling and is closely associated with asthma severity. These ASMCs also synthesize and secrete excessive extracellular matrix proteins, resulting in inappropriate extracellular matrix deposition in the airway walls and aggravating airway stiffness and stenosis [6]. The pathogenic mechanisms underlying ASMC abnormality remain incompletely understood.

Therapeutic approaches to reversing and correcting these changes are very limited. For example, thermoplastic brachioplasty has been used to treat patients with severe asthma by reducing ASMC mass and airway hyperresponsiveness. However, some asthma patients respond poorly to this therapy [7]. Glucocorticoids

(GCs), the major anti-inflammatory drug utilized in treating asthma, only partially reverse ASMC proliferation and hypertrophy [8,9]. Long-acting β-adrenoceptor agonists have little effect on reversing the proliferation and hypertrophy of ASMCs, although they can alleviate ASMC contraction [10]. Therefore, a better understanding of ASMC growth regulation during asthmatic inflammation has become a key for developing new therapeutic approaches [11].

Smooth muscle cell differentiation is characterized by the sequential appearance of cytoskeletal and contractile proteins. Expression of these contractile genes is coordinated by a serum response factor (SRF)-dependent transcriptional complex through binding to a DNA sequence motif $CC(A/T)_6GG$ (CArG box) in the promoters of multiple smooth muscle contractile genes [12]. However, ubiquitously expressed SRF can form the active transcriptional complex only when bound to lineage-restricted co-activator Myocd (also called myocardin) or its family members (MRTF-A and MRTF-B) [13]. Deletion of *Myocd* or *Mrtfb* during embryonic development could result in a severe deficiency of smooth muscle cells *in vivo* [14]. Interestingly, deletion of *Myocd* in embryonic lung mesenchymal progenitors using the Tbx4 lung enhancer-driven Tet-On inducible Cre results in deficiency of smooth muscle formation only in the airways, not in the vasculature [15]. This suggests that distinct mechanisms have evolved to regulate Myocd activity in airway versus vascular smooth muscle cell development and response to injury. Therefore, we hypothesized that Myocd might play a critical role in controlling ASMC remodeling in asthma. To test this hypothesis, *Myocd* was deleted specifically in mouse lung mesenchymal cells after postnatal lung development using the same Tbx4 lung enhancer-driven Cre, and these mice were challenged with chronic allergic stimuli. By comparing the asthmatic pathology between these *Myocd* conditional knockout mice and the wild-type (WT) controls, we found that Myocd was an important transcriptional regulator involved in ASMC remodeling and asthma progression.

Materials and methods

Mice

Tbx4-rtTA/TetO-Cre transgenic mice were generated in our lab [16]. Floxed-*Myocd* (*Myocd*^fl/fl^) mice were provided by Dr. Michael Parmacek [17]. Timed mating was carried out between *Tbx4-rtTA/TetO-Cre/ Myocd*^fl/+^ and *Myocd*^fl/fl^ mice, and mouse genotypes were determined by genomic DNA PCR following the aforementioned published methods. The pups with desired genotypes at 1 month of age were fed doxycycline (Dox) chow (625 mg/kg) and drinking water (0.5 mg/ml) for 4 weeks to induce Cre-mediated *Myocd* deletion. Mice with double allele deletion of *Myocd* were referred to as conditional knockout (CKO), while all mice without any *Myocd* deletion were simply grouped as WT controls. Both male and female mice (about 1:1) were used in each group. All mice were bred on the C57BL/6J strain background and housed in specific pathogen-free conditions at the animal facility of Children's Hospital Los Angeles. The studies followed the NIH Animal Research Advisory Committee Guidelines (https://oacu.oir.nih.gov/animal-research-advisory-committee-arac-guidelines, last accessed 20 December 2020), and all procedures were approved by the Institutional Animal Care and Use Committee at Children's Hospital Los Angeles.

Mouse asthma model: establishment and testing

Ovalbumin (OVA) solution (Sigma-Aldrich, St. Louis, MO, USA) was prepared in PBS and emulsified with an equal volume of aluminum hydroxide adjuvant (Imject Alum, ThermoFisher, Waltham, MA, USA). One week after the last day of Dox induction, the mice received an intraperitoneal injection of OVA (25 mg/50 µl) for initial sensitization (day 0). The OVA injection was then repeated on day 14. Control mice were injected with an equal volume of sterile PBS only. These sensitized mice were then challenged with 25 µg of OVA in 50 µl PBS through noninvasive intratracheal delivery 5 days a week starting at day 21 (Figure 1). After 4 weeks of continuous OVA challenge, either pulmonary function tests were performed or lung specimens, including bronchoalveolar lavage fluid (BALF) and tissues, were collected 24 h after the last OVA stimulation. The isolated lung tissues were either fixed in 4% buffered paraformaldehyde or flash-frozen in liquid nitrogen.

Histology and morphometric analysis

Lung tissues were inflated under 25 cm H_2O pressure through intratracheal cannulation prior to fixation. The fixed tissues were embedded in paraffin wax and sectioned at 5-µm thickness. These tissue sections were used for hematoxylin and eosin (H&E) staining and immunofluorescence staining to detect cellular markers using the methods described previously [18]. In brief, antigen retrieval was performed by boiling the deparaffinized and rehydrated tissue sections in Tris-EDTA buffer (pH 9.0) for 30 min. After blocking in 10% donkey serum for 1 h, the tissue sections were incubated with the following primary antibodies overnight at 4 °C: 1:3,000 dilution of mouse anti-Acta2 (A2547; Sigma Aldrich), 1:200 dilution of rat anti-Cdh1 (14-3249-82, Thermo Fisher), or 1:600 dilution of rabbit anti-Ki67 (122025, Cell Signaling Technology, Danvers, MA, USA). After washing, the slides were incubated with 1:600 dilution of donkey secondary antibodies conjugated with Alexa Fluor 488, Alexa Fluor 594, or Alexa Fluor 647 (Thermo Fisher) for 1 h. The cell nuclei were counterstained using DAPI in the mounting medium (Vector Laboratories, Newark, CA, USA). Fluorescence 2D images were captured using a Zeiss LSM710 confocal microscope at the Imaging Core Facility of Children's Hospital Los Angeles. The area of
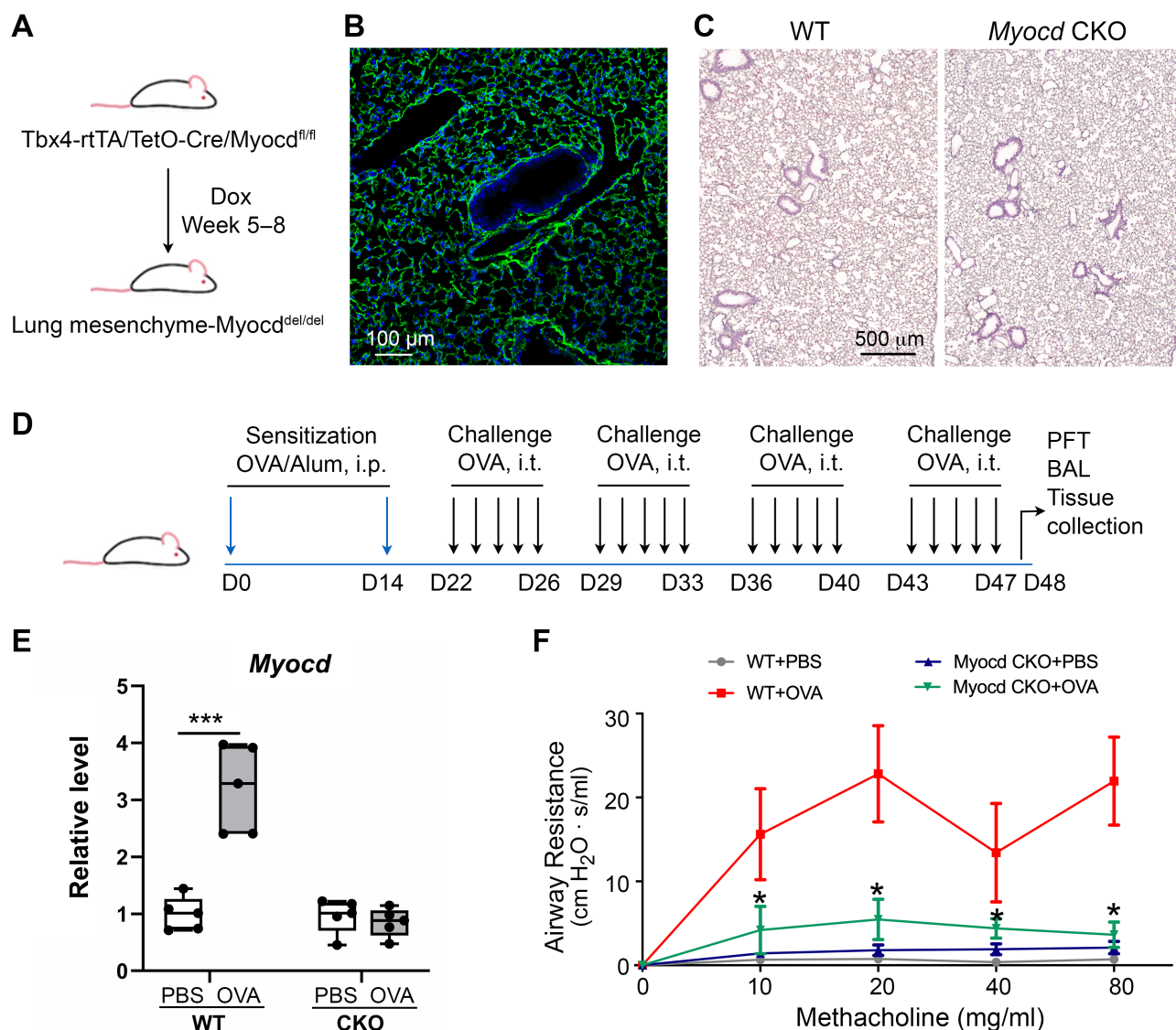
Figure 1. Postdevelopmental deletion of *Myocd* in lung mesenchyme attenuates allergen-induced airway hyperresponsiveness. (A) CKO of *Myocd* was induced by Dox administration from 5 to 8 weeks of age in mice with the indicated genotypes. (B) Dox-induced Cre expression was validated by mGFP expression in the mTmG reporter mouse lung. (C) Lung tissue morphology was compared between WT and *Myocd* CKO mice. (D) Procedures to establish a chronic asthmatic mouse model. D, day; i.p., intraperitoneal injection; it, intratracheal installation. (E) Comparison of *Myocd* expression at mRNA level between different mouse lung tissues; ***$p < 0.001$. (F) Airway hyperresponsiveness to methacholine was compared among different groups as indicated (mean ± SEM, $n > 4$, *$p < 0.05$).

peri-airway Acta2-positive smooth muscles and the number of cell nuclei in the Acta2-positive area were measured using ImageJ software (https://imagej.nih.gov/ij/index.html, last accessed 5 March 2022). The area was normalized by dividing by the airway basement membrane length in each measurement as previously reported [19]. The hypertrophic index is the airway muscle area divided by the total number of smooth muscle cell nuclei and normalized using basement membrane length [20]. Similarly, proliferating ASMCs were positively stained for both Acta2 and Ki67 (Acta2$^+$/Ki67$^+$), and the proliferative index was calculated by dividing the number of Ki67$^+$ ASMCs with total ASMCs (DAPI$^+$) [21]. At least four lungs per genotype and condition were analyzed. Results were analyzed using two-way ANOVA to compare

the differences between mean values and were considered significant if $p < 0.05$.

BALF collection and analysis

Bronchoalveolar lavage (BAL) was performed as described in a previous publication [22]. In brief, the mouse trachea was cannulated with a 20G plastic catheter. Sterile PBS (600 μl) was instilled and recovered and repeated three times. The cells in the combined BAL fluid were quantified using a hemocytometer and loaded onto microscope slides by cytospin (4 min at 800 rpm). After staining with Hema 3 (Thermo Fisher), the percentage of different inflammatory cells in BAL fluid were calculated by counting 300 leukocytes in randomly

selected fields under an oil lens of Zeiss Axioscope with ×630 overall magnification [23]

Inflammation score

H&E-stained lung tissue sections were examined for peribronchiolar, perivascular, and alveolar inflammation under the microscope, following a method published previously [24,25]. At least 10 randomly selected fields were scanned in each sample. The peribronchiolar and perivascular inflammation were scored (0–4): 0, normal; 1, few inflammatory cells; 2, a ring of inflammatory cells with one cell layer deep; 3, a ring of inflammatory cells with two to four cell layers deep; 4, a ring of inflammatory cells of more than four cells deep. In addition, the numerical scores (0–5) for alveolar inflammation were determined as follows: 0, normal; 1, alveolar walls normal, few macrophages in alveoli; 2, mild thickening of alveolar walls and increased alveolar macrophages and eosinophils; 3, marked thickening of alveolar walls and alveolar multinucleated giant cells and eosinophils in 30–50% of the field; 4, changes as in 3 but with >50% of the field; 5, complete consolidation.

Quantitative measurement of cytokine mRNAs

Total RNA was isolated from mouse lung tissue using the RNeasy kit (Qiagen, Germantown, MD, USA) and reverse-transcribed into cDNA using the iScript™ cDNA Synthesis Kit (Bio-Rad, Hercules, CA, USA). Real-time PCR amplification was conducted using the SYBR Green Q-PCR kit on an iCycler-iQ system (Bio-Rad), as described previously [26]. Each sample was run in triplicate, and PCR reactions without the addition of the template were used as blank controls. The primer sequences for *Il4*, *Il13*, *Tnf*, and *Tgfb1* are listed in the supplementary material, Table S1. The amount of cDNA templates per reaction was normalized using *Actb* expression as a reference, and the relative expression of the target gene as compared to the WT-PBS samples was calculated by the ΔΔCT method [27].

Quantification of fibrillar collagen

Collagens were stained with Picro-Sirius Red to enhance birefringence of co-aligned collagen fibers. When viewed with polarizing microscope, only crosslinked fibrillar collagen exhibits yellow-red color of birefringence from the dark background of the lung tissues. The captured birefringence signal was then converted into grayscale regardless of the original colors and quantified using ImageJ [18]. The fibrillar collagen area was then normalized for airway size [fibrillar collagen area (μm^2)/airway epithelial perimeter (μm)].

Measurement of airway mucus expression

Mucin expression was assessed by counting under a microscope the total number of periodic acid–Schiff (PAS)-positive and PAS-negative epithelial cells in 10 random airways (with diameters of approximately 100–150 μm) in each mouse lung section. Results were expressed as the percentage of PAS-positive cells per airway [28].

Mouse pulmonary function tests

Lung function test was performed using FlexiVent (SciReq, Montréal, QC, Canada) following a published method [25]. In brief, the mouse was deeply anesthetized by intraperitoneal injection of euthasol (0.25 ml/kg body weight, which is equivalent to pentobarbital 97.5 mg/kg body weight). In a supine position, an intratracheal catheter was placed through a tracheotomy, and the mouse was ventilated. The pulmonary function was measured following the protocol provided by the manufacturer.

Statistical analyses

Quantitative differences among multiple groups with different genotypes and different allergic challenges were analyzed using two-way ANOVA, followed by Bonferroni multiple comparison tests. Results are expressed as mean ± SEM; $p < 0.05$ was considered significant.

Results

Abrogation of lung mesenchymal Myocd mitigates airway hyperresponsiveness in an OVA-induced chronic allergic asthma mouse model

As reported previously [15], Myocd is essential for airway smooth muscle development. To determine the role of Myocd in regulating ASMC remodeling in adulthood, we generated mice with the genotypes of *Tbx4-rtTA/TetO-Cre/Myocd*$^{fl/fl}$ and induced lung mesenchyme-specific deletion of *Myocd* postnatally by administering Dox to the mice from the age of postnatal 5 weeks to 8 weeks (Figure 1A). The *Tbx4-rtTA/TetO-Cre* transgenic mice had Dox-inducible Cre expression specifically in lung mesenchymal cells [16], and Cre induction in adult mouse lung mesenchymal cells including ASMCs was validated by the Cre-mediated membrane GFP (mGFP) expression of the mTmG dual fluorescence reporter (Figure 1B). Abnormal structures of both airways and alveoli were not observed in the *Myocd* CKO lungs compared to those of WT mice under normal conditions (Figure 1C). The adult mice with lung mesenchymal *Myocd* CKO and their WT littermates were then used to generate a chronic allergic asthma model by sensitizing and challenging them with OVA for 4 weeks (Figure 1D) since chronic OVA challenge but not acute OVA stimulation to OVA-sensitized mice has been shown to induce ASMC hypertrophy [20]. *Myocd* expression at the mRNA level was significantly increased in WT lungs upon repeated OVA challenges, whereas the *Myocd* mRNA level was not altered between lungs with OVA challenges and PBS controls in *Myocd* CKO mice (Figure 1E). Airway hyperresponsiveness, an integrated measurement for asthma clinical

response, was measured using FlexiVent and compared among the groups with different *Myocd* genotypes and allergic challenges (Figure 1F). The increase of airway resistance in responding to methacholine (10–80 mg/ml) was significantly attenuated in *Myocd* CKO mice compared to WT mice that received OVA challenges, suggesting that blockade of Myocd function during chronic allergen exposure mitigates airway hyperresponsiveness.

Myocd knockout inhibits asthmatic ASMC hypertrophy and hyperplasia in the chronic allergic asthma model

To understand the cellular mechanisms underlying the attenuated airway resistance described earlier, we then compared the changes in ASMCs among mice with different *Myocd* genotypes and exposure conditions. ASMCs and proliferating cells were detected by airway Acta2 and Ki67 coimmunostaining (Figure 2A) and quantitatively measured using ImageJ software. All calculated ASMC values were normalized by the underlying length of the basement membrane. The normalized average area of the ASMC layer in *Myocd* CKO lungs was significantly decreased compared to WT mouse lungs with the same chronic challenge of OVA allergen ($2.163 \pm 0.484 \ \mu m^2/\mu m$ versus $10.100 \pm 2.392 \ \mu m^2/\mu m$, $p < 0.01$ in Figure 2B). Similarly, the normalized hypertrophy index (ASMC-area/ASMC-number/basement membrane length), which reflects the average size of individual ASMC, was significantly reduced in OVA-challenged *Myocd*
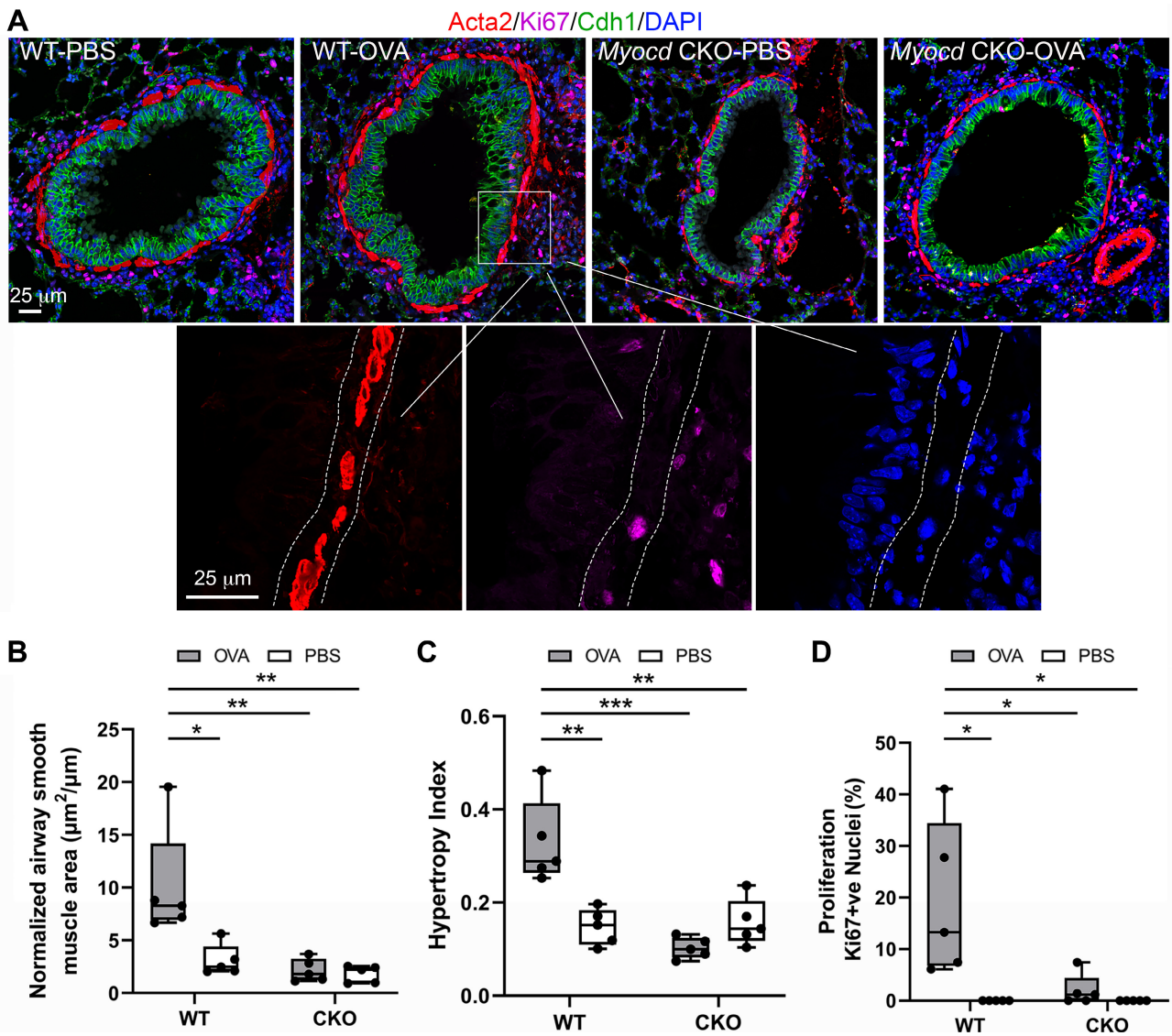

Figure 2. Comparison of airway smooth muscle cells (ASMCs) in OVA-induced asthmatic mouse lungs between *Myocd* CKO and WT groups. (A) ASMCs were identified by Acta2 immunostaining (red) and proliferating ASMCs were recognized by Ki67 coimmunostaining (magenta). Airway epithelial cells were marked by Cdh1 costaining (green), and all nuclei were counterstained by DAPI (blue). The ASMC layer at greater magnification is shown in the inserts, highlighted by dotted lines. (B–D) Comparison of normalized average area of ASMC layers, normalized ASMC hypertrophy index, and normalized ASMC proliferation index among different groups. There were five mice in the WT-OVA and CKO-OVA groups, and four mice in the WT-PBS and CKO-PBS groups. *$p < 0.05$, **$p < 0.01$, ***$p < 0.001$.

CKO lungs compared to OVA-challenged WT lungs (0.103 ± 0.010 μm^2/μm versus 0.329 ± 0.041 μm^2/μm, $p < 0.001$ in Figure 2C). Moreover, proliferation of ASMCs in the *Myocd* CKO-OVA group was significant decreased compared to the WT-OVA group ($2.002 \pm 1.389\%$ versus $19.127 \pm 6.699\%$, $p < 0.05$ in Figure 2D). This suggests that deletion of Myocd inhibits chronic allergic responses of ASMCs by inhibiting the abnormal increases in ASMC number and size.

Allergen-induced airway inflammation was also reduced in the lungs of mice with mesenchymal-specific knockout of *Myocd*

Airway inflammation and remodeling are the major pathological changes seen in chronic asthmatic lungs. Therefore, we also evaluated inflammatory alterations in the lungs of *Myocd* CKO mice. Examination of the BALF revealed that the number of total cells in BALF from *Myocd* CKO-OVA mouse lungs was relatively reduced compared to the number of BALF cells from WT-OVA mouse lungs ($3.171 \times 10^5 \pm 0.459 \times 10^5$ versus $11.340 \times 10^5 \pm 2.123 \times 10^5$, $p < 0.001$, Figure 3A). However, the profiles of inflammatory cell types were similar between BALFs of WT-OVA and *Myocd* CKO-OVA lungs (Figure 3B–D), although the total numbers of these cells were significantly decreased in *Myocd* CKO-OVA BALF (eosinophils: $0.768 \times 10^5 \pm 0.360 \times 10^5$, lymphocytes: $1.326 \times 10^5 \pm 0.510 \times 10^5$, macrophages: $1.422 \times 10^5 \pm 0.450 \times 10^5$) compared to WT-OVA BALF (eosinophils: $2.420 \times 10^5 \pm 1.520 \times 10^5$, lymphocytes: $5.188 \times 10^5 \pm 2.610 \times 10^5$, macrophages: $6.716 \times 10^5 \pm 2.880 \times 10^5$).

We examined lung tissue sections for inflammation. Massive infiltration by inflammatory cells (mainly mononuclear cells) was seen in the peri-airway areas of the WT-OVA group. However, inflammatory cell infiltration around the airways was attenuated in the *Myocd* CKO-OVA group (Figure 4A). Using a semiquantitative scoring system as published previously [24,25], we evaluated the inflammatory response in different anatomic locations including the peribronchiolar region, the perivascular

region, and the peripheral alveolar region. Consistent with the histological changes, the inflammatory response in the parabronchiolar region was significantly reduced in *Myocd* CKO-OVA lungs compared to WT-OVA lungs (2.382 ± 0.105 versus 3.480 ± 0.081, $p < 0.05$ in Figure 4B), while inflammation in the perivascular and alveolar regions (3.76 ± 0.093 versus 3.904 ± 0.043, $p > 0.05$ and 2.300 ± 0.063 versus 2.264 ± 0.050, $p > 0.05$, respectively) was similar between these two OVA groups (Figure 4C,D). In addition, mRNA expression of proinflammatory cytokines, including *Il4* and *Il13* (Th2 cytokines) as well as *Tnf*, was decreased in *Myocd* CKO-OVA lungs compared to WT-OVA lungs (Figure 4E–G). Altered expression of other growth factor mRNAs, such as *Tgfb1*, was not detected (Figure 4H). Therefore, our results suggest that lung mesenchyme-specific deletion of Myocd not only inhibits abnormal airway smooth muscle remodeling but also attenuates airway inflammation.

Mesenchymal deletion of *Myocd* attenuated deposition of fibrillar collagen in asthmatic airways

Increased collagen deposition in the airway wall is one of the pathological changes observed in asthma [29]. Prolonged allergen exposure has been shown to enhance collagen deposition in the airways of the rat asthma model [30]. Consistent with these findings, we observed increased fibrillar collagen deposition in the asthmatic airways of WT mice (Figure 5A), as detected by Picro-Sirius Red staining and visualized under polarized light using our previously published method [18,31]. Interestingly, mesenchymal deletion of *Myocd* significantly mitigated the deposition of fibrillar collagen in the OVA-challenged airways, as validated by semiquantitative measurement for the area of airway fibrillar collagen and normalization with the internal perimeter of airway lining epithelia (2.673 ± 0.706 μm^2/μm in *Myocd* CKO versus 12.205 ± 3.939 μm^2/μm in WT, $*p < 0.05$ in Figure 5B). This suggests that deletion of Myocd in lung mesenchymal cells also inhibits prolonged allergen-induced airway collagen deposition, directly
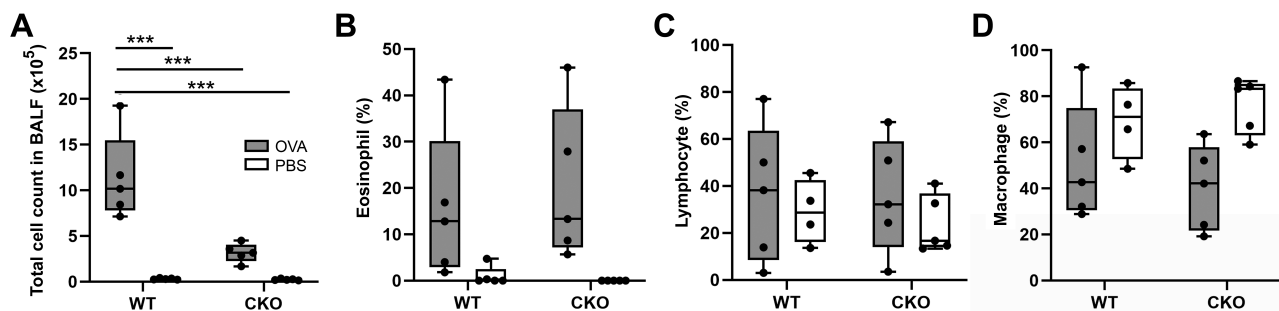

Figure 3. Alteration of inflammatory cells in bronchoalveolar lavage fluid of *Myocd* CKO lungs. Bronchoalveolar lavage fluid was collected from the mouse 24 h after the last challenge. (A) With the same OVA challenge, the total cell numbers in the BALF recovered from *Myocd* CKO mouse lungs was significantly decreased compared to those from WT mice. However, the cell composition (B, C, and D) of BALF, measured as percentages of eosinophils, lymphocytes, and macrophages, was not significantly different between *Myocd* CKO and WT mice. $n = 5$, ***$p < 0.001$.
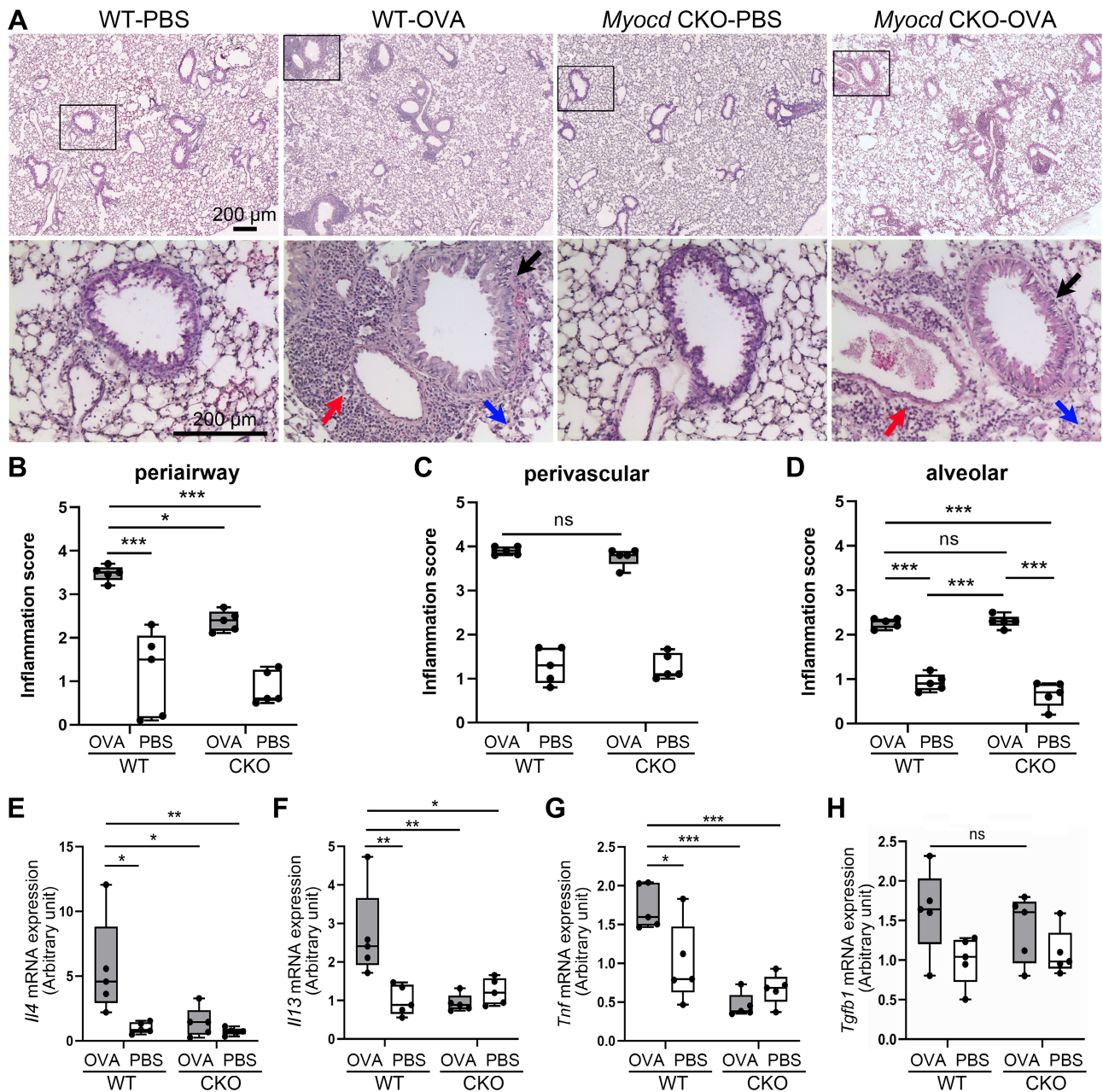
Figure 4. Lung mesenchymal *Myocd* deletion reduced OVA-induced lung inflammation. (A) Inflammation assessment of lung tissue sections with H&E staining: massive infiltration of inflammatory cells was seen in peri-airway (black arrow), perivascular (red arrow), and alveolar structures (blue arrow) of OVA-challenged WT mouse lungs compared to those in PBS-treated WT controls. In contrast, the severity of inflammatory cell infiltration in *Myocd* CKO lungs, particularly in the peri-airway area, was reduced. (B–D) Inflammatory infiltration in peri-airway, vascular, and alveolar regions was separately evaluated using a semiquantitative scoring method. Significant difference was detected for peri-airway inflammation (2.382 ± 0.236 versus 3.480 ± 0.182, *$p < 0.05$), but not for perivascular and alveolar inflammation between OVA-treated WT and *Myocd* CKO groups. Five mice were included in each group, and 10 randomly selected fields were evaluated for each mouse. Ns, no significance. *$p < 0.05$, **$p < 0.01$, ***$p < 0.001$. (E–H) Expression of asthma-related cytokine/growth factor mRNAs *Il4*, *Il13*, *Tnf*, and *Tgfb1* was determined by RT-qPCR and presented relative to WT-PBS samples ($n = 5$, *$p < 0.05$, **$p < 0.01$, ***$p < 0.001$). *Actb* was used as a reference transcript for normalization.

through ASMCs and/or indirectly through other mesenchymal cells.

Allergen-induced airway epithelial mucin overexpression was significantly reduced in mesenchymal *Myocd* knockout lungs

Airway mucus hypersecretion is another pathological feature of chronic asthma [32]. In particular, colloidal mucus plugs in the airways are associated with mortality in severe asthma [33]. Mucins are the main components in mucus, which are a group of heavily glycosylated proteins produced by epithelial cells. Using PAS staining, mucin overproduction was easily detected in WT mouse airway epithelial cells after OVA treatment (Figure 6A). However, production of mucins was significantly reduced in the airway epithelial cells of OVA-challenged lungs with mesenchyme-specific *Myocd* knockout. This was also
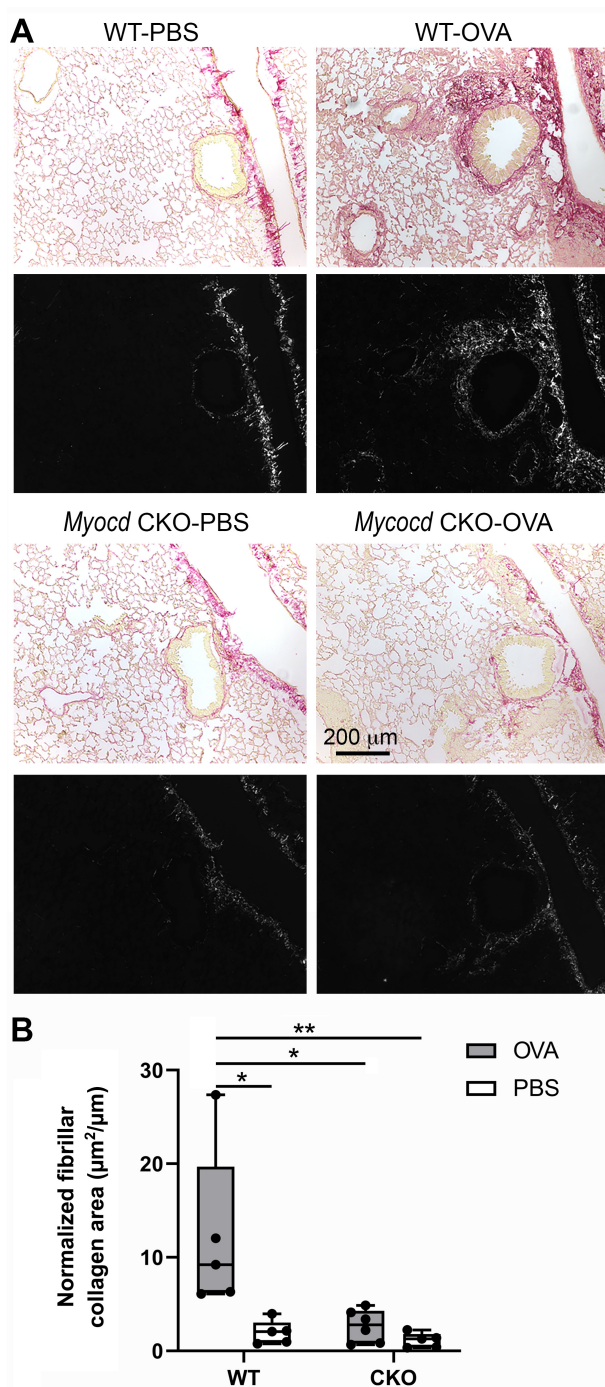
Figure 5. Lung mesenchyme-specific knockout of *Myocd* reduced prolonged OVA treatment-induced fibrillar collagen deposition in airway walls. (A) Picro-Sirius Red staining of lung tissue sections of indicated genotypes and allergen challenges viewed under bright field and polarized light microscopy, respectively. The captured birefringence signal under polarizing microscopy was converted into grayscale and quantified using ImageJ. The PBS group was used as normal control. (B) Semiquantitative measurement of the area of fibrillar collagen deposition in airways was performed for more than five fields per sample, five or six samples per condition, and normalized by the internal perimeter of airway epithelium. *$p < 0.05$, **$p < 0.01$.

Figure 6. Deletion of mesenchymal *Myocd* inhibited mucin expression in airway epithelial cells under prolonged allergen exposure. (A) PAS-staining of lung tissue sections with different genotypes and allergen exposures. Increased mucin expression was obvious in OVA-challenged WT lung airway epithelial cells, but subtle in OVA-challenged *Myocd* CKO lung airway epithelia. (B) The percentage of cells that were PAS-positive was calculated per bronchiole and compared. ***$p < 0.001$ ($n > 5$ per group).

Discussion

Previous studies found that mesenchymal knockout of *Myocd* during fetal lung development results in severe deficiency in ASMC growth, suggesting that Myocd plays an essential role in promoting airway smooth muscle development [15]. However, the specific roles of

supported by quantifying PAS-positive epithelial cells in the airways (Figure 6B). Therefore, mesenchymal Myocd not only participates in allergen induced ASMC remodeling but also affects epithelial mucin expression.
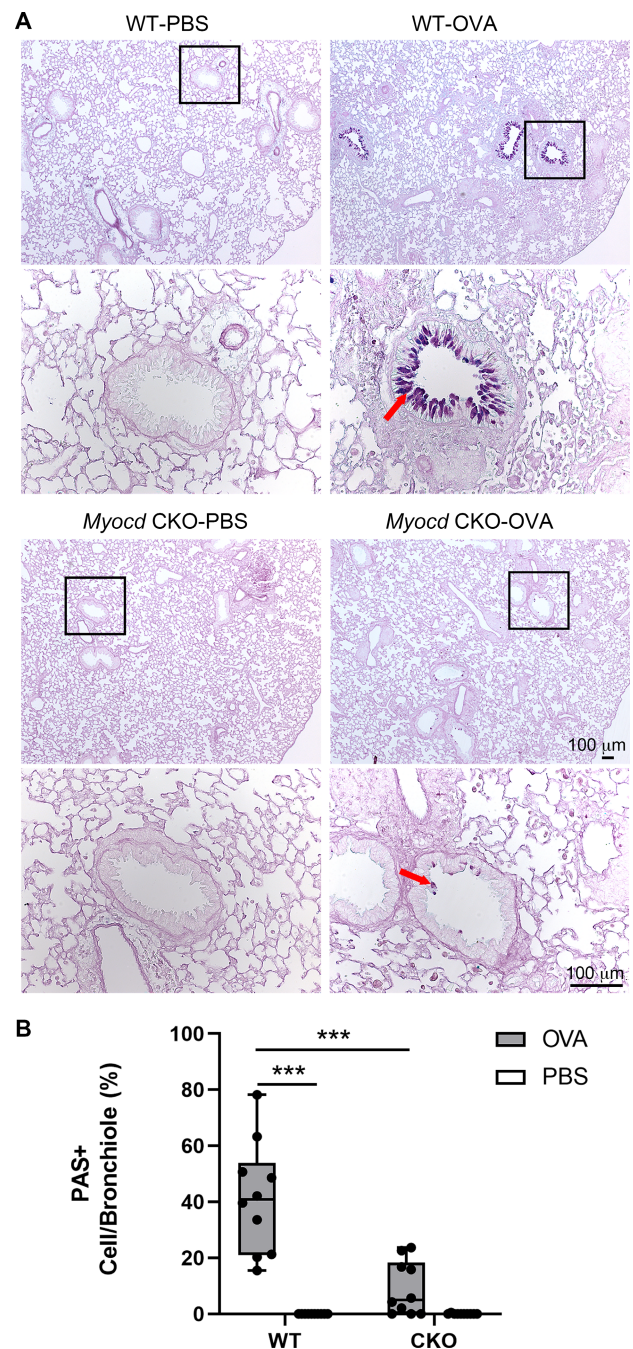
Myocd in maintaining and repairing ASMCs under either physiological or pathological conditions during postnatal life have not been investigated. In an OVA-induced chronic asthma mouse model, we have demonstrated for the first time that genetic deletion of *Myocd* in postnatal lung mesenchymal cells mitigates allergen-induced abnormal airway remodeling and reduces airway hyperresponsiveness, accompanied by decreased peri-airway inflammation and airway epithelial mucus production.

As described earlier, Myocd is a transcriptional coactivator that binds SRF, which drives smooth muscle contractile gene expression by promoting a stable ternary complex formation on the CArG box of these gene promoters. During asthmatic airway remodeling, Myocd may interact with SRF and other cofactors such as pElk-1, leading to ASMC hypertrophy and hyperplasia in asthmatic airways [34]. The upstream molecular pathways remain elusive. Abnormal RhoA/ROCK activation has been reported to be associated with airway hyperresponsiveness and airway remodeling [35], and treatment of bronchial smooth muscle cells with IL-13 results in the upregulation of RhoA [36,37]. Consistent with this observation, inhibition of RhoA/ROCK signaling alleviates allergen-induced ASMC contraction, airway wall thickening, and subepithelial collagen deposition in asthma animal models [38–42]. In aortic vascular smooth muscle cells, increased ROCK activation is associated with the upregulation of SRF and *Myocd* expression [43]. It is reasonable to postulate that RhoA/ROCK regulates Myocd activation and/or expression [13], which will need to be investigated in the future.

The mechanisms underlying the distinct role of Myocd in promoting smooth muscle cell growth in pulmonary airways, but not in pulmonary vasculature, remain unclear. MRTF-A and MRTF-B are the two additional transcriptional coactivators for SRF-mediated smooth muscle cell growth, which may compensate for Myocd deficiency in some cells such as vascular smooth muscle cells [44]. Another possibility is that the Tbx4-driven Cre expression in pulmonary vasculature is not sufficient after development [16], which would result in inefficiency of Cre-mediated floxed-*Myocd* deletion in the vascular smooth muscle cells.

In addition, the deposition of collagen around the asthmatic airway was significantly decreased in the *Myocd* CKO-OVA lungs compared to the WT-OVA lungs. Abnormal deposition of collagen underneath the basement membrane and increased stiffness of the airway wall can be attributed to ASMC remodeling. Conversely, collagen type I enhances growth factor induced ASMC proliferation [45]. Therefore, abnormal ASMC remodeling is mediated not only by cytokine-stimulated cellular changes but also by excessive extracellular matrix production-induced phenotype switching. Interestingly, inhibition of MRTF-A/SRF signaling was reported to increase fibroblast apoptotic susceptibility and reduce TGF-β-induced myofibroblast differentiation *in vitro* and to attenuate collagen deposition in mouse lung fibrosis models [46].

In our chronic asthma mouse model, we also show that reduction of airway remodeling has an inhibitory effect on lung inflammation, particularly around the airways. Previous studies have shown that ASMCs are capable of producing several cytokines (including IL-13, IL-5, IL-8, and TNF), chemokines, and cell adhesion molecules, which subsequently influence the airway inflammatory response and airway remodeling by recruiting more inflammatory cells and autocrine-induced ASMC contraction, gene expression, and proliferation [47–50]. We found a significant reduction in Th2 type cytokines (IL-4 and IL-13) and TNF in the lungs of the OVA-challenged *Myocd* CKO mice compared to the WT mice, which is correlated with reduced AMSC abnormal phenotype. As discussed earlier, these proinflammatory cytokines can activate RhoA/ROCK signaling and downstream SRF/Myocd complex activity. In addition, deletion or inhibition of *Mrtfa* (previously known as *Mkl1*) was reported to reduce vascular inflammation [51]. Therefore, allergen-induced chronic inflammation and abnormal ASMC response constitutes a vicious cycle that exacerbates asthmatic airway abnormality, and inhibition of ASMC abnormal remodeling is important for stopping the progression of asthmatic pathology.

In addition to inflammation–ASMC remodeling, we also observed the interaction between airway epithelial cells and ASMCs in our chronic asthma mouse model. Mucin production in airway epithelial cells was increased in OVA-challenged WT lungs, while a significant reduction in mucin-positive airway epithelial cells was seen in OVA-challenged *Myocd* CKO lungs, indicating that mitigation of ASMC remodeling also has an indirect effect on airway epithelial cells. It has been reported that abnormal ASMCs secrete CCL20, which in turn binds to CCR6 on epithelial cells and induces mucus production in epithelial cells [52]. In addition, as adjacent cells, ASMCs are also affected by the growth factors released from epithelial cells in altering cell proliferation, differentiation, and inflammatory regulation [53]. Therefore, ASMC–epithelial interaction also plays an important role in chronic asthma development, and our study suggests a central role of ASMCs in affecting airway epithelial pathology.

In summary, our study showed that abnormal ASMC remodeling plays central roles in chronic asthma airway pathology by affecting airway thickness and stiffness, the inflammatory response, and epithelial hyperplasia and dysfunction. Myocd is a key transcriptional coactivator involved in ASMC pathological changes in a chronic asthma model. Inhibition of Myocd activity in ASMCs may provide a new approach to breaking the vicious cycle of asthmatic progression and become a novel target in treating severe and persistent asthma.

Acknowledgements

Author contributions statement

QY, QM and WS contributed to study concept and design. QY, QM, YL, HC, DL, JC, HW and MC acquired data. QY, QM, YL, MC, MP and WS analyzed and interpreted the data. QY, QM, JC, MP and WS drafted and edited the manuscript. All authors approved the final version of the manuscript.

Data availability statement

The data supporting the conclusions of this article are included in this publication and/or its supplementary material.

References

1. Joseph C, Tatler AL. Pathobiology of airway remodeling in asthma: the emerging role of Integrins. *J Asthma Allergy* 2022; **15:** 595–610.
2. Payne DN, Rogers AV, Adelroth E, *et al*. Early thickening of the reticular basement membrane in children with difficult asthma. *AmJRespirCrit Care Med* 2003; **167:** 78–82.
3. Andersson CK, Iwasaki J, Cook J, *et al*. Impaired airway epithelial cell wound-healing capacity is associated with airway remodelling following RSV infection in severe preschool wheeze. *Allergy* 2020; **75:** 3195–3207.
4. Banno A, Reddy AT, Lakshmi SP, *et al*. Bidirectional interaction of airway epithelial remodeling and inflammation in asthma. *Clin Sci (Lond)* 2020; **134:** 1063–1079.
5. Khan MA. Inflammation signals airway smooth muscle cell proliferation in asthma pathogenesis. *Multidiscip Respir Med* 2013; **8:** 11.
6. Ijpma G, Panariti A, Lauzon AM, *et al*. Directional preference of airway smooth muscle mass increase in human asthmatic airways. *Am J Physiol Lung Cell Mol Physiol* 2017; **312:** L845–L854.
7. Menzella F, Lusuardi M, Galeone C, *et al*. Bronchial thermoplasty and the role of airway smooth muscle: are we on the right direction? *Ther Clin Risk Manag* 2017; **13:** 1213–1221.
8. Keglowich LF, Borger P. The three A's in asthma - airway smooth muscle, Airway Remodeling & Angiogenesis. *Open Respir Med J* 2015; **9:** 70–80.
9. Leclere M, Lavoie-Lamoureux A, Joubert P, *et al*. Corticosteroids and antigen avoidance decrease airway smooth muscle mass in an equine asthma model. *Am J Respir Cell Mol Biol* 2012; **47:** 589–596.
10. Hirst SJ, Martin JG, Bonacci JV, *et al*. Proliferative aspects of airway smooth muscle. *J Allergy Clin Immunol* 2004; **114:** S2–S17.
11. Prakash YS, Halayko AJ, Gosens R, *et al*. An official American Thoracic Society research statement: current challenges facing research and therapeutic advances in airway remodeling. *Am J Respir Crit Care Med* 2017; **195:** e4–e19.
12. Owens GK, Kumar MS, Wamhoff BR. Molecular regulation of vascular smooth muscle cell differentiation in development and disease. *Physiol Rev* 2004; **84:** 767–801.
13. Yang Q, Shi W. Rho/ROCK-MYOCD in regulating airway smooth muscle growth and remodeling. *Am J Physiol Lung Cell Mol Physiol* 2021; **321:** L1–L5.
14. Parmacek MS. Myocardin-related transcription factors: critical coactivators regulating cardiovascular development and adaptation. *Circ Res* 2007; **100:** 633–644.
15. Young RE, Jones MK, Hines EA, *et al*. Smooth muscle differentiation is essential for airway size, tracheal cartilage segmentation, but dispensable for epithelial branching. *Dev Cell* 2020; **53:** 73–85.e75.
16. Zhang W, Menke DB, Jiang M, *et al*. Spatial-temporal targeting of lung-specific mesenchyme by a Tbx4 enhancer. *BMC Biol* 2013; **11:** 111.
17. Huang J, Cheng L, Li J, *et al*. Myocardin regulates expression of contractile genes in smooth muscle cells and is required for closure of the ductus arteriosus in mice. *J Clin Invest* 2008; **118:** 515–525.
18. Luo Y, Xu W, Chen H, *et al*. A novel profibrotic mechanism mediated by TGFβ-stimulated collagen prolyl hydroxylase expression in fibrotic lung mesenchymal cells. *J Pathol* 2015; **236:** 384–394.
19. Hirota JA, Ellis R, Inman MD. Regional differences in the pattern of airway remodeling following chronic allergen exposure in mice. *Respir Res* 2006; **7:** 120.
20. Plant PJ, North ML, Ward A, *et al*. Hypertrophic airway smooth muscle mass correlates with increased airway responsiveness in a murine model of asthma. *Am J Respir Cell Mol Biol* 2012; **46:** 532–540.
21. Hassan M, Jo T, Risse PA, *et al*. Airway smooth muscle remodeling is a dynamic process in severe long-standing asthma. *J Allergy Clin Immunol* 2010; **125:** 1037–1045.e1033.
22. Zhao J, Shi W, Wang YL, *et al*. Smad3 deficiency attenuates bleomycin-induced pulmonary fibrosis in mice. *Am J Physiol Lung Cell Mol Physiol* 2002; **282:** L585–L593.
23. Ikeda RK, Nayar J, Cho JY, *et al*. Resolution of airway inflammation following ovalbumin inhalation: comparison of ISS DNA and corticosteroids. *Am J Respir Cell Mol Biol* 2003; **28:** 655–663.
24. Ford JG, Rennick D, Donaldson DD, *et al*. Il-13 and IFN-gamma: interactions in lung inflammation. *J Immunol* 2001; **167:** 1769–1777.
25. Xu W, Lan Q, Chen M, *et al*. Adoptive transfer of induced-Treg cells effectively attenuates murine airway allergic inflammation. *PLoS One* 2012; **7:** e40314.
26. Luo Y, El Agha E, Turcatel G, *et al*. Mesenchymal adenomatous polyposis coli plays critical and diverse roles in regulating lung development. *BMC Biol* 2015; **13:** 42.
27. Shi W, Chen H, Sun J, *et al*. TACE is required for fetal murine cardiac development and modeling. *Dev Biol* 2003; **261:** 371–380.
28. Cho JY, Miller M, Baek KJ, *et al*. Immunostimulatory DNA sequences inhibit respiratory syncytial viral load, airway inflammation, and mucus secretion. *J Allergy Clin Immunol* 2001; **108:** 697–702.
29. Roche WR, Beasley R, Williams JH, *et al*. Subepithelial fibrosis in the bronchi of asthmatics. *Lancet* 1989; **1:** 520–524.
30. Palmans E, Pauwels RA, Kips JC. Repeated allergen exposure changes collagen composition in airways of sensitised Brown Norway rats. *Eur Respir J* 2002; **20:** 280–285.
31. Tarantal AF, Chen H, Shi TT, *et al*. Overexpression of transforming growth factor-beta1 in fetal monkey lung results in prenatal pulmonary fibrosis. *Eur Respir J* 2010; **36:** 907–914.
32. Johnson DC. Airway mucus function and dysfunction. *N Engl J Med* 2011; **364:** 978.
33. Kuyper LM, Paré PD, Hogg JC, *et al*. Characterization of airway plugging in fatal asthma. *Am J Med* 2003; **115:** 6–11.
34. Chevigny M, Guérin-Montpetit K, Vargas A, *et al*. Contribution of SRF, Elk-1, and myocardin to airway smooth muscle remodeling in heaves, an asthma-like disease of horses. *Am J Physiol Lung Cell Mol Physiol* 2015; **309:** L37–L45.
35. Zhang Y, Saradna A, Ratan R, *et al*. RhoA/Rho-kinases in asthma: from pathogenesis to therapeutic targets. *Clin Transl Immunology* 2020; **9:** e01134.
36. Chiba Y, Tanabe M, Goto K, *et al*. Down-regulation of miR-133a contributes to up-regulation of Rhoa in bronchial smooth muscle cells. *Am J Respir Crit Care Med* 2009; **180:** 713–719.
37. Han X, Yang F, Cao H, *et al*. Malat1 regulates serum response factor through miR-133 as a competing endogenous RNA in myogenesis. *FASEB J* 2015; **29:** 3054–3064.
38. Ke X, Do DC, Li C, *et al*. Ras homolog family member A/Rho-associated protein kinase 1 signaling modulates lineage commitment of mesenchymal stem cells in asthmatic patients through lymphoid

enhancer-binding factor 1. *J Allergy Clin Immunol* 2019; **143**: 1560–1574.e6.

39. Wei B, Shang YX, Li M, *et al*. Cytoskeleton changes of airway smooth muscle cells in juvenile rats with airway remodeling in asthma and the RhoA/ROCK signaling pathway mechanism. *Genet Mol Res* 2014; **13**: 559–569.

40. Yoshii A, Iizuka K, Dobashi K, *et al*. Relaxation of contracted rabbit tracheal and human bronchial smooth muscle by Y-27632 through inhibition of Ca^{2+} sensitization. *Am J Respir Cell Mol Biol* 1999; **20**: 1190–1200.

41. Chiba Y, Ueno A, Shinozaki K, *et al*. Involvement of RhoA-mediated Ca^{2+} sensitization in antigen-induced bronchial smooth muscle hyperresponsiveness in mice. *Respir Res* 2005; **6**: 4.

42. Chiba Y, Takada Y, Miyamoto S, *et al*. Augmented acetylcholine-induced, Rho-mediated Ca^{2+} sensitization of bronchial smooth muscle contraction in antigen-induced airway hyperresponsive rats. *Br J Pharmacol* 1999; **127**: 597–600.

43. Zhou N, Lee JJ, Stoll S, *et al*. Rho kinase regulates aortic vascular smooth muscle cell stiffness via actin/SRF/Myocardin in hypertension. *Cell Physiol Biochem* 2017; **44**: 701–715.

44. Pipes GC, Creemers EE, Olson EN. The myocardin family of transcriptional coactivators: versatile regulators of cell growth, migration, and myogenesis. *Genes Dev* 2006; **20**: 1545–1556.

45. Dekkers BG, Spanjer AI, van der Schuyt RD, *et al*. Focal adhesion kinase regulates collagen I-induced airway smooth muscle phenotype switching. *J Pharmacol Exp Ther* 2013; **346**: 86–95.

46. Sisson TH, Ajayi IO, Subbotina N, *et al*. Inhibition of myocardin-related transcription factor/serum response factor signaling decreases lung fibrosis and promotes mesenchymal cell apoptosis. *Am J Pathol* 2015; **185**: 969–986.

47. Hakonarson H, Maskeri N, Carter C, *et al*. Autocrine interaction between IL-5 and IL-1beta mediates altered responsiveness of atopic asthmatic sensitized airway smooth muscle. *J Clin Invest* 1999; **104**: 657–667.

48. Sampson AP. The role of eosinophils and neutrophils in inflammation. *Clin Exp Allergy* 2000; **30**: 22–27.

49. Camoretti-Mercado B, Lockey RF. Airway smooth muscle pathophysiology in asthma. *J Allergy Clin Immunol* 2021; **147**: 1983–1995.

50. Tliba O, Panettieri RA. Noncontractile functions of airway smooth muscle cells in asthma. *Annu Rev Physiol* 2009; **71**: 509–535.

51. Gao P, Zhao J, Shan S, *et al*. MKL1 cooperates with p38MAPK to promote vascular senescence, inflammation, and abdominal aortic aneurysm. *Redox Biol* 2021; **41**: 101903.

52. Faiz A, Weckmann M, Tasena H, *et al*. Profiling of healthy and asthmatic airway smooth muscle cells following interleukin-1β treatment: a novel role for CCL20 in chronic mucus hypersecretion. *Eur Respir J* 2018; **52**: 1800310.

53. O'Sullivan MJ, Jang JH, Panariti A, *et al*. Airway epithelial cells drive airway smooth muscle cell phenotype switching to the proliferative and pro-inflammatory phenotype. *Front Physiol* 2021; **12**: 687654.

SUPPLEMENTARY MATERIAL ONLINE

Table S1. DNA primers used for qPCR